



Lifetime study in advanced isolation techniques

A. Poyai^{*,1}, E. Simoen, C. Claeys¹, R. Rooyackers, G. Badenes

IMEC, Kapeldreef 75, B-3001 Leuven, Belgium

Abstract

The impact of different isolation schemes on the p–n junction characteristics is compared. From the diode current–voltage behaviour, the silicon generation and recombination lifetime is extracted. It will be shown that the recombination lifetime is higher in the case of shallow trench isolation (STI) than in the case of polysilicon encapsulated local oxidation of silicon (PELOX). The opposite trend is observed for the generation lifetime. These results will be discussed in view of the defects present in the p-well of the diodes, which are studied by other spectroscopic and microscopic techniques. © 2001 Elsevier Science Ltd. All rights reserved.

Keywords: STI; PELOX; Lifetime; Isolation

1. Introduction

With the continuing reduction of device dimensions in CMOS technology, the impact of the isolation process on device performance becomes increasingly important. This is related to the increased mechanical stress associated with aggressive isolation schemes like shallow trench isolation (STI) and Polysilicon encapsulated local oxidation (PELOX), suitable for (sub)quarter micron CMOS. The stress may affect the electrical device performance, like diode junction leakage, in different ways. Either directly or when exceeding the silicon yield stress, by the creation of extended defects [1,2]. Here, the lifetime properties of shallow junctions with different isolation schemes will be compared. In order to assess the process-induced defects, diode measurements are combined with structural and spectroscopic measurement techniques.

2. Experimental

Shallow n⁺–p diodes compatible with submicron CMOS technology have been processed in a p-well,

fabricated on 150 mm p-type substrates. STI or PELOX are used for isolation. A retrograde p-well is made by a deep ($1.2 \times 10^{13} \text{ cm}^{-2}$ at 200 keV) and a shallow ($1.5 \times 10^{13} \text{ cm}^{-2}$ at 55 keV) boron ion implantation, followed by a dopant activation anneal (10 min, 850°C). The n⁺ region is obtained by arsenic ion implantation ($4 \times 10^{15} \text{ cm}^{-2}$ at 70 keV) and anneal (10 s, 1100°C). Finally, cobalt-silicidation was applied, using an 8 nm Ti cap layer. The maximum silicidation temperature for the STI wafers was 700°C, compared with 750°C for the PELOX batch. Current–voltage (*I*–*V*) measurements have been done on diodes with different geometry. Also temperature (*T*) dependent measurements were performed in the range 25–120°C, allowing extraction of the activation energy of the reverse current density.

3. Results and discussion

In order to study the different geometrical current components, diodes with different area (*A*), perimeter (*P*) and number of corners (*N_C*) have been investigated. Beside rectangular (“square” SQ) diodes also meander (ME) or perimeter diodes have been included in the study. Combining a number of SQ and ME diodes that allow to separate the volume or bulk current density *J_A* (A/cm²) which scales with the diode area, from the

^{*}Corresponding author. Fax: +32-16-281-214.

E-mail address: amporn@imec.be (A. Poyai).

¹Also at E.E. Department, KU Leuven, Leuven, Belgium.

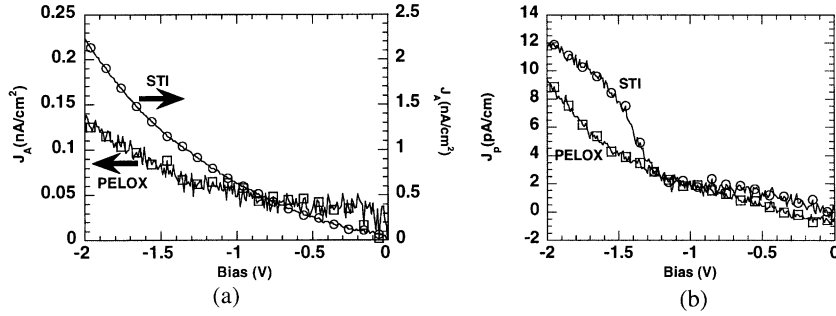


Fig. 1. Area (a) and peripheral (b) current density versus reverse bias with different isolation.

peripheral density J_P (A/cm), assumed proportional with P . In principle, also a corner component J_C (A/corner) can be separated. The separation of the geometrical current components is based on the assumption that the total reverse current I_R is a linear combination of the different contributions, given by

$$I_R = AJ_A + PJ_P + N_C J_C + I_{\text{par}}. \quad (1)$$

As is seen from Eq. (1), at least four different geometry diodes have to be measured to separate the different components. I_{par} represents the parasitic sample-independent system leakage. In principle, the same separation scheme can be applied for the forward current density J_F or for the junction capacitance [3]. Applying Eq. (1) to the set of diodes, the area and peripheral current density can be separated as shown in Fig. 1.

Fig. 1 shows that the area and peripheral leakage current density are higher in STI than in PELOX. The peripheral component is believed to be directly affected by the isolation scheme. It is clear that in order to obtain tolerable J_P levels of around a few pA/cm, the current STI process needs further optimisation. The area leakage component, on the other hand, is not directly impacted by the isolation, but depends on the defects present in the p-well region. In order to analyse these more carefully, the recombination and generation lifetime is derived next from the forward and reverse $I-V$ characteristic, respectively.

The area diffusion current density (J_{dA}) can be obtained from the forward $I-V$ characteristic by taking the ideality factor into account. The results are summarized in Table 1. The area diffusion current density is higher in PELOX than STI. Assuming that the diffusion current in the n^+-p diodes is dominated by the diffusion of electrons in the p-well region, the recombination lifetime (τ_r) can be calculated from the following equation:

$$\tau_r = \left(\frac{qn_i^2}{J_{dA} N_A} \sqrt{D_n} \right)^2, \quad (2)$$

where q is the elementary charge, n_i is the intrinsic carrier concentration, N_A is the acceptor density and D_n

Table 1

P-well concentration (N_A), area diffusion current density (J_{dA}), recombination lifetime (τ_r), effective generation lifetime (τ_g) at -1 V, effective activation energy (E_A) at -1 V, in STI and PELOX diodes

Isolation	N_A (cm $^{-3}$)	J_{dA} (A/cm 2)	τ_r (ps)	τ_g (μ s)	E_A (eV)
STI	2.51×10^{17}	1.37×10^{-11}	145	32.7	0.268
PELOX	2.53×10^{17}	2.48×10^{-11}	43.3	833.0	0.353

the diffusion coefficient of electrons. The resulting recombination lifetime is summarized in Table 1. Such low values either point to a high density of traps in the p-well region or indicate that our basic assumption is not correct and that hole diffusion and recombination in the neutral n^+ region dominate the diffusion current. In order to decide on the exact mechanism, the generation lifetime has been derived from the reverse area current density.

Normally, the area leakage current density in a p-n junction can be explained by the following equation:

$$J_A = J_{dA} + \frac{qn_i}{\tau_g} W_A, \quad (3)$$

where W_A is the area depletion width and τ_g the generation lifetime. Knowing the area diffusion current density from the forward $I-V$ characteristic and the area depletion width from the area capacitance, the effective generation lifetime at different reverse bias can be obtained as shown in Fig. 2a and the values at -1 V are summarized in Table 1. The effective generation lifetime is higher in PELOX than STI, which is opposite to the recombination lifetime trend. This strongly suggests that the area diffusion current in the shallow n^+-p junctions studied is governed by the hole transport in the top layer. In addition, the ratio of both lifetimes (τ_g/τ_r) is so high that an unrealistic energy level is derived from it. In order to have a better idea of the defect level position in the bandgap, the leakage current is studied as a function of the temperature T . From an

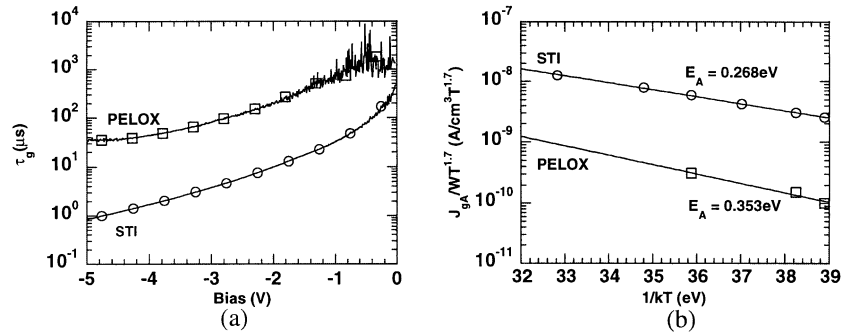


Fig. 2. (a) Effective generation current versus reverse bias at 25°C and (b) Arrhenius plot of the area generation current density of diode with different isolation.

Arrhenius plot, the activation energy of the generation current is derived, which is related to the trap level position E_t .

By taking the area depletion width temperature dependence into account, the temperature variation of the area generation current density is given by

$$\frac{J_{gA}}{W_A} = BT^{1.7} \exp\left(-\frac{E_A}{kT}\right), \quad (4)$$

where B is a constant, E_A is the effective activation energy and k is the Boltzmann constant [4]. The effective activation energy can be found from the Arrhenius plots of Fig. 2b, corresponding to a reverse bias of -1 V . The E_A values at -1 V for the different isolation schemes are summarized in Table 1. Normally, a value around 0.56 eV (the intrinsic Fermi level) is expected for the activation energy of the generation current. The data obtained here indicate that the responsible generation centres have an energy level that is closer to one of the band edges. The fact that for STI a lower activation energy is found indicates that the generation centres are less efficient than for PELOX. The leakage current is higher, however, which could point to a much higher trap density N_T .

Further identification of the defects has been obtained from deep level transient spectroscopy (DLTS) studies on the same diodes. In brief, the following observations have been made: all diodes show a broad distribution of energy levels in the range $0.3\text{--}0.5\text{ eV}$ above the valence band (hole traps). However, for the STI case, the hole traps have on the average a higher activation energy and trap concentration. This is not consistent with the leakage current results. Furthermore, from trap level profiling, it has been derived that the defects are not uniformly distributed in the depletion region, extending in the p-well. A peak of trap concentration around $0.2\text{ }\mu\text{m}$ depth below the junction has been found. The fact that the traps are distributed both in energy and in depth points to the existence of point defect clusters in the p-well. These could originate for example from the

deep B ion implantation used to fabricate the p-well. Unfortunately, these clusters could not be seen by transmission electron microscopy. In addition, it has become clear that also the details of the silicidation play a role in the defect formation. This follows from a comparison of the “high” temperature results (PELOX) with the “low” temperature STI case, although the exact defect generation mechanism is not resolved for the moment. It is well known that silicidation may inject vacancies, which can be trapped by the interstitial species, causing the disappearance of the interstitial-related levels [5].

4. Conclusions

The peripheral current component is impacted by the isolation technique, while the area current component is governed by the process-induced defects.

Acknowledgements

A. Poyai is indebted to the Thai government for his scholarship supported through the National Science and Technology Development Agency (NSTDA) of Thailand.

References

- [1] Kuroi T, Uchida T, Horita K, Sakai M, Itoh Y, Inoue Y, Nishimura T. International Electron Devices Meeting (IEDM) 1998;98:141.
- [2] Smeys P, Griffin PB, Rek ZU, De Wolf I, Saraswat KC. IEEE Trans Electron Devices 1999;46:1245.
- [3] Czerwinski A, Simoen E, Claeys C, Klima K, Tomaszewski D, Gibki J, Katcki J. J Electrochem Soc 1998;145:2107.
- [4] Aharoni H, Ohmi T, Oka MM, Nakada A, Tamai Y. J Appl Phys 1997;81:1270.
- [5] Mathiot D. Appl Phys Lett 1991;58:131.